Sādhanā (2022) 47:134
https://doi.org/10.1007/s12046-022-01904-4

Development and characterization of copper doped perovskite-polymer composite through high-temperature technique

PRIYAMBADA MALLICK[1], RASHMIRANJAN PATRA[1], DEBABRATA MOHANTY[2] and SANTOSH KU. SATPATHY[1,*]

[1]Centurion University of Technology and Management, Bhubaneswar, Odisha, India
[2]Yuan Ze University, Taoyuan City, Taiwan
e-mail: santosh.satpathy@cutm.ac.in

MS received 16 August 2021; revised 8 February 2022; accepted 11 May 2022

Abstract. Ceramic powders of Cu doped lead Titanate ($Pb_{0.5}Cu_{0.5}TiO_3$) are synthesized through a solid-state reaction method at high-temperature. Different percentage of ceramic filler into the polymer matrix was prepared by solution casting techniques. The structural studies of this polymeric composite were characterized by the X-ray diffraction technique and a tetragonal phase was found. Moreover, the surface morphology of this material was done by scanning electron microscopy. The impedance studies of this polymeric composite were characterized by an LCR meter between the frequencies range 10^2 and10^6 Hz. The modulus study of the material was done between the frequency ranges 10^2 and10^6 Hz. The variation of ac conductivity with frequency at different temperatures satisfied Jonscher's universal power law.

Keywords. Solid-state reaction; polymer; dielectric constant; AC conductivity; impedance.

1. Introduction

Among ferroelectric perovskite materials (ABO_3), Lead Titanate ($PbTiO_3$) is a mostly researched material because of its unique physical structure and several other significant properties. These materials show a high value of the dielectric constant, low dielectric loss, high electrical resistivity, and good electrical properties. Because of their excellent piezoelectric and electrical properties, these are ideal for various applications in the fields of thin-film capacitors, electronic transducers, pyroelectric sensors, and nonlinear optics. These materials exhibit spontaneous polarization and can also switch the direction of polarization [1]. $PbTiO_3$ shows a relatively low value of dielectric constant ($\sim$200) with a high curie temperature (about 490°C) [2] as compared to its other family members like Barium Titanate ($BaTiO_3$) and Lead Zirconate (PZT) ceramics due to which it is widely used in space navigation industry and medical engineering. It has a high value of pyroelectric coefficient and relatively low permittivity which makes it an ideal material for the application of pyroelectric infrared detectors, space light modulator, total-internal reflection optical switch, and other electronic devices [3]. At ambient temperature, it shows a strong anisotropy which may be as high as $\sim$1.6 (c/a ratio). A large value of the c/a ratio favors the enhanced electrical properties [4]. Also, perovskite-polymer composites have been ideal for photovoltaic applications and solar cells. It shows improved power conversion efficiency of 20.06% [5]. In recent years, a group of researchers has found ideal white light with chromaticity coordination at 0.3379 and 0.3432 and color temperature of 5261 K from inorganic perovskite quantum dots- polymer composites [6]. Several studies suggested that halide perovskite quantum dots (QD) composites can be used in photocatalytic applications to convert CO_2 into solar fuels in nonaqueous media [7]. The perovskite solar cells are flexible, easy to fabricate, and can be prepared at low temperatures. Ferroelectric ceramic-polymer composites have drawn much attention because of their high dielectric constant and low loss as well as insulating nature [8].

Ferroelectric materials possess a high dielectric constant but they are brittle and difficult to fabricate in bulk whereas, in the case of polymers, they are flexible and also have a low loss. Hence the ferroelectric perovskite ceramic-polymer composite will have an improved dielectric constant with a low loss which will make it ideal for various electronics applications as well as the flexible nature will make the fabrication work much easier task [9]. On the other hand, Poly (methyl methacrylate) (PMMA) is a suitable polymer for the work of the polymer matrix. It is insulating in nature with a low dielectric constant of nearly 4.9 with a low loss [10]. So the composite made from this polymer may have a low loss with

*For correspondence
Published online: 06 July 2022

an enhanced dielectric constant due to the presence of ceramic filler in it.

In this work, we synthesized copper doped Lead Titanate, then used this ceramic powder as fillers to the polymer matrix and prepared ceramic-polymer composites by the solution casting method. Dopant Cu can enhance the dielectric constant, electrical conductivity, and carrier mobility of these films [11]. Again, a good doping phase enables the material for various applications. In our previous papers [12–17], we have already discussed the doping of rare earth or transition metals in different perovskite materials and also investigated the modification in the dielectric and electrical properties of the samples. Here, we adopted a conventional solid-state reaction method to synthesize the material i.e. Cu doped lead titanate ($Pb_{0.5}Cu_{0.5}TiO_3$) because most of the chemical-based processing routes require organic or organometallic chemicals of high purity which are much more expensive than the oxides which are also widely available. Here we focus on the dielectric and electrical properties of the composite. The transport properties of the material are also studied with the help of complex permittivity (ε^*), complex impedance (Z^*), and dielectric loss ($\tan\delta$).

2. Experimental technique

Here we have prepared the Cu doped $PbTiO_3$ ceramic powder by using ingredients of high purity (98%) in stoichiometric quantity with the help of the high-temperature solid-state method. The ingredients were weighed by the stoichiometry method and blended carefully. The blending was first done in an air medium for 2 h and after that, the same was followed for another 2 h in an alcoholic medium. The mixture was then kept in a pure alumina crucible and calcinated in an oven at a temperature of 950°C for 4 h. The formation of the compound was confirmed by using the X-ray diffraction (XRD) technique. The ferroelectric ceramic-polymer composites were prepared using a solution casting technique. At first, the ceramic powder was taken in a crucible according to weight percentage and heated for two hours with a temperature of 150°C. Then the powder was ground for 30 min. Then 20 ml of N, N-Dimethylformamide was taken in a conical flask and 5 g of PMMA was added to it. The mixture was left at ambient temperature for 20 min under continuous stirring by using a magnetic stirrer until a homogenous mixture was formed. Then, to the above mixture stoichiometric amount of ceramic powder ($Pb_{0.5}Cu_{0.5}$) TiO_3 was added. Again, the mixture was stirred for 2 h and a homogeneous mixture was obtained. Then the homogeneous mixture was placed on a glass petri dish in a hot air oven at 120°C for 4–5 h. Finally, the polymer-ceramic composite film was obtained. The composites were coated with a silver paste of high purity and dried at 100°C for the sake of electrical measurements. The formation, as well as structural properties of the composites, were studied by X-ray diffraction (Rigaku, Ultima IV). Dielectric and impedance measurements were performed using an LCR meter computed (Impedance analyzer, IM 3570).

3. Result and discussion

3.1 *Structural study*

The structural study was done by X-ray diffraction. The XRD patterns of the composites having different ceramic concentrations (5%, and 10%) are shown in figure 1 from which the tetragonal perovskite structure is confirmed for all the concentrations with lattice constant listed in table 1. A strong peak is observed for the doped material (Cu). The crystallite size is calculated from the widening of the XRD peaks by using the Scherrer equation

$$D = K\lambda/\left(\beta_{1/2}Cos\theta_{hkl}\right) \tag{1}$$

where K = 0.89, λ = 1.5406 Å, $\beta_{1/2}$ = Full width of the reflection at half of the maximum intensity [18].

From table 1, we can observe that the lattice constant (a, b, c) obtained by using the Diffract Eva software is decreasing with an increase in the crystallite size which is well-matched with the literature [19]. Here, a strong doping phase (Cu phase) can be observed for each of the samples which will make the composites ideal for various industrial applications.

From table 2, it is noticed that with a rise in the ceramic amount in the polymer matrix, the crystallinity of the polymer is increasing. It also shows the average crystallite size of particles in the composite decreases with an increase in ceramic percentage.

The microstrain (ε) for all the samples was calculated by the relation [20]

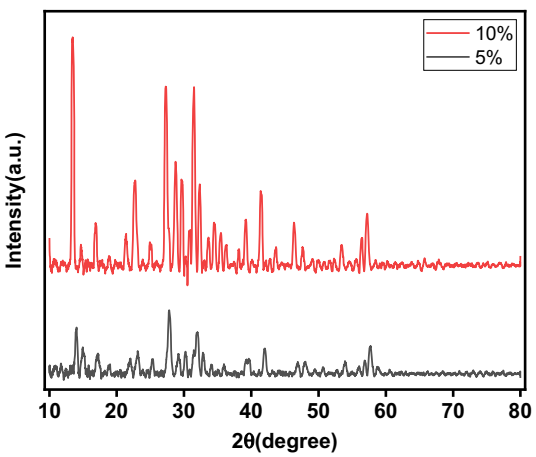

Figure 1. XRD pattern of composite films at the different ceramic filler concentrations.

Table 1. Lattice constants of composite films according to filler percentage.

No.	Filler percentage	a (Å)	b (Å)	c (Å)
1	5	3.9	3.9	4.15
2	10	4.6	4.6	4.73

Table 2. Structural Study by XRD.

No.	Filler %age	Average crystallite size (nm)	Avg. dislocation density [δ] $\times 10^{-3}$ (nm^{-2})	Avg. micro strain [$\varepsilon \times 10^{-3}$]	Crystallinity (%)
1	5	17	3.7	0.39	3.2
2	10	16	3.6	0.37	3.9

$$\varepsilon = \left(\frac{\lambda}{D\cos\theta} - \beta\right)\left(\frac{1}{\tan\theta}\right) \tag{2}$$

where the symbols represent their usual meanings. The length of dislocation lines present per unit volume of the crystal is referred to as the dislocation density which can be evaluated using the Williamson and Smallman's relation [21]

$$\delta = \frac{1}{D^2} \tag{3}$$

where δ signifies the dislocation density. We have prepared a ceramic-polymer composite, so there must be an amorphous phase along with the crystalline phase. So, the degree of crystallinity of the films is calculated with the help of the equation [22].

$$Crystallinity = \frac{Area\ of\ the\ crysttaline\ peaks}{Area\ of\ all\ peaks(crystalline + amorphous)} \times 100 \tag{4}$$

The findings of structural studies are listed in table 2 from which it can be observed that with an increase in the ceramic percentage in the material, the average crystallite size, the average dislocation density, and the average microstrain decreases while the crystallinity increases.

3.2 *Microstructural study*

The microstructural study was done by the SEM study as shown in figure 2. The homogenous dispersion of ceramic fillers in the polymer matrix is noticed. It can be observed that with a rise in the ceramic percentage in the composite, the homogeneity of the composites decreases. This may be due to the agglomeration of the ceramic particles when added in a higher amount into the polymer matrix.

3.3 *Dielectric study*

From the variation of dielectric constant (ε_r) with frequency as shown in figure 3, it is noticed that the dielectric constant attains a maximum value at low frequency, and then decreases gradually with a rise in frequency. The dielectric constant has a large value at a low-frequency range which is due to the presence of more than one type of polarization in this region like atomic, ionic, interfacial, and electronic polarization while in the high-frequency region only the electronic polarization occurs which affects the value of dielectric constant resulting in a decrease of dielectric constant [23].

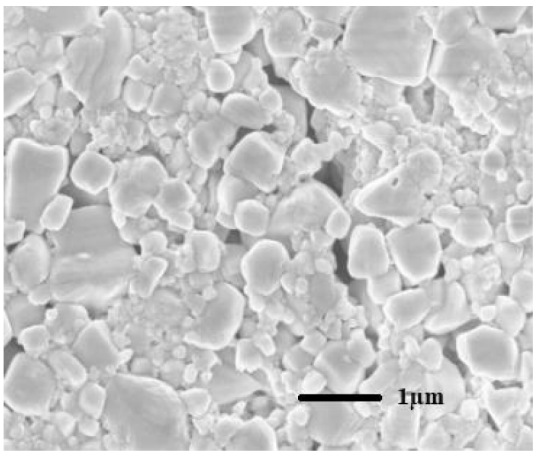

(a) 5%

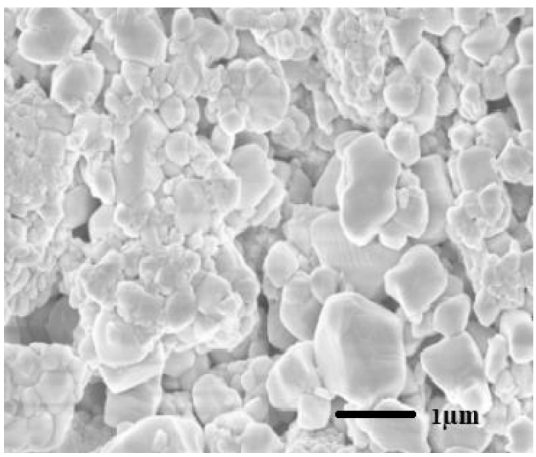

(b) 10%

Figure 2. (**a**) and (**b**) SEM image of composite films with 5% and 10% of ceramic filler.

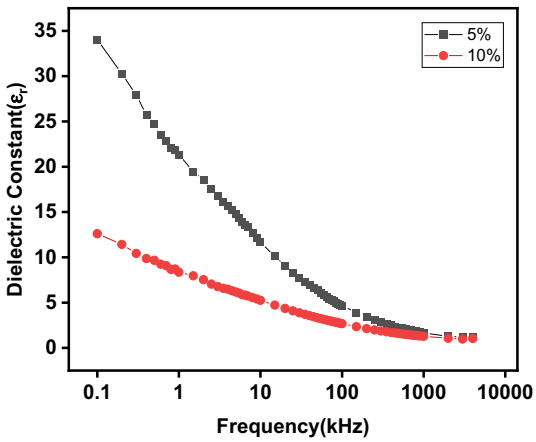

Figure 3. Frequency variation of dielectric constant (ε_r) of composite films with 5% and 10% ceramic filler.

Figure 3 also shows that on a rise in the ceramic filler concentration in the polymer matrix, the value of the dielectric constant decreases. It is observed that the highest value of the dielectric constant is found to be 34.02 at 100 Hz for the composite film having a 5% filler percentage. For 10% filler, the dielectric constant is found to be 12.6 at 100 Hz. The variation of the Dielectric constant according to the ceramic filler concentration can be studied based on their ratio between phase transformation to the lattice parameter [24].

Again, the variation of dielectric loss (tan δ) with frequency is shown in figure 4. For the lower frequency range, it shows a high loss. As the frequency increases, the value of tanδ starts to decrease. The orientational polarization and the electrical conductivity of material may affect the dielectric loss. The high value of tan δ at a lower frequency may result in the high resistivity of the grain boundary. Here a single relaxation peak is observed in all the samples which may be due to the occurrence of ionic conduction in the system. Here, the frequency of the electric field and the rotating frequency of the molecule are coordinating, hence,

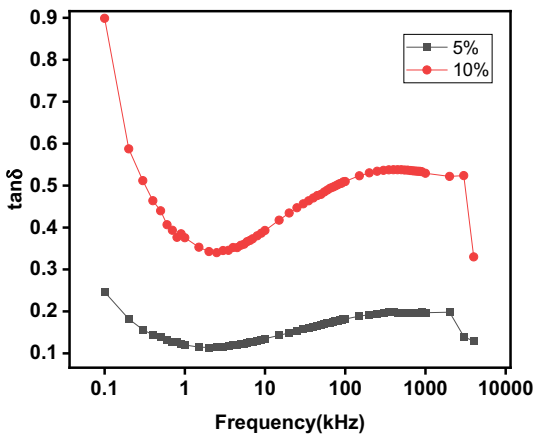

Figure 4. Frequency variation of dielectric loss composite films with 5% and 10% ceramic filler.

for each of the samples, at a particular frequency, maxima can be seen [25]. Since the dielectric constant of the materials is linearly proportional to the average value of grain size, the decrease of dielectric constant and tan δ as a result of Cu doping is due to the decrease in grain size. This confirms that the doping of Cu has affected the fabrication of $PbTiO_3$ ceramics. This explains the mobility of grain boundary decreases because of the separation of defects created due to doping near the grain boundary [26]. As the ceramic concentration increases in the polymer matrix, the loss also increases. The observed dielectric loss for 5% and 10% of ceramic polymer films in the frequency range of 1 to 10 kHz are 0.114, 0.33 respectively which is considerably low.

In 2012, Pascariu *et al* [27] showed that the $PbTiO_3$-Epoxy resin composite thick films have a dielectric constant value ranging from 5 to 12 with a low loss whereas in our work we are getting a much-increased value of dielectric constant with a low loss which is good from the perspective of dielectric applications. It shows that the doping of Cu influenced the dielectric properties of the composite. Tamboli *et al* [28] in 2014 revealed that PMMA-BFO composites can have a dielectric constant value $\sim$14 while in our work we are getting a dielectric constant value more than twice of the earlier which indicates that the addition of $PbCuTiO_3$ surely enhanced the dielectric constant. Several other pieces of literature have also shown similar values of dielectric constant and loss which is well supporting our work. The synthesis process, crystal structure, dielectric constant, and loss values from similar works along with the current work are listed in table 3.

3.4 *Impedance study*

To analyze the transport properties and nature of the material response, a study of complex impedance is used [33] to understand the real and imaginary parts of impedance, modulus parameters.

From figure 5, we can analyze the variation of the real part of impedance with frequency. It shows that the value of the real part of impedance decreases with an increase in frequency and attains a saturation value at a higher frequency region. The decrease in the value of the real part of impedance with decreased content of ceramic means for a ceramic-polymer composite film having a lower concentration of ceramic can possess a high value of ac conductivity. Relatively low-value saturation frequency indicates that heavier ion/dipole may be associated with some switching. This suggests the presence of a mixed nature of polarization behavior in the material, such as electronic, ionic, and orientation polarization. These results indicate a possibility of an increase in ac conductivity which is due to the release of space charge and lowering in the barrier properties of the material.

Table 3. Comparison of dielectric properties.

Name	Sample	Doping	Method	Structure	Dielectric constant	Loss	References
Synthesis and characterization of Cu doped perovskite materials	$PbTiO_3$ (polymer film) (this work)	CuO	Solid-state, solution casting	Tetragonal	34.0299	0.114	This work
Ferroelectric polymer-ceramic composite thick films For energy storage applications	$Pb(Zr_{0.52}Ti_{0.48})\ O_3$ (PVDF-PZT) (polymer-ceramic composite thick films)	No doping	Solid state.	Tetragonal	~25	<0.1	[29]
Dielectric studies and AC conductivity of piezoelectric barium titanate ceramic Polymer composites	Barium titanate (ceramic polymer composite thin films)	No doping	Solution casting	Pseudo-cubic	47.8, 63.4, and 39.5	~0.1	[30]
Fabrication and dielectric properties of the $BaTiO_3$–polymer Nano-composite thin films	$BaTiO_3$ (polymer nano-composite thin films)	No doping	Complex alkoxide method	Cubic	31.8	0.05	[31]
Preparation and characterization Of $PbTiO_3$–epoxy resin compositionally Graded thick films	$PbTiO_3$ (composite thick films)	No doping	Solid state, gravity casting method	Tetragonal	5–12	0.233–0.023	[27]
Polymethyl methacrylate (PMMA)–bismuth ferrite (BFO) nanocomposite: low loss and high dielectric constant materials with perceptible magnetic properties	BFO (Nanocomposites)	No doping	Auto combustion method, in-situ polymerization method	Rhombohedral	~ 14	0.037	[28]
fabrication of $BaTiO_3$-Pmma polymer nanocomposite thin/ thick films and their dielectric properties	$BaTiO_3$ (nanocomposite thin/thick films)	No doping	Hydrothermal/solvothermal route	Cubic, tetragonal	9	0.04	[32]

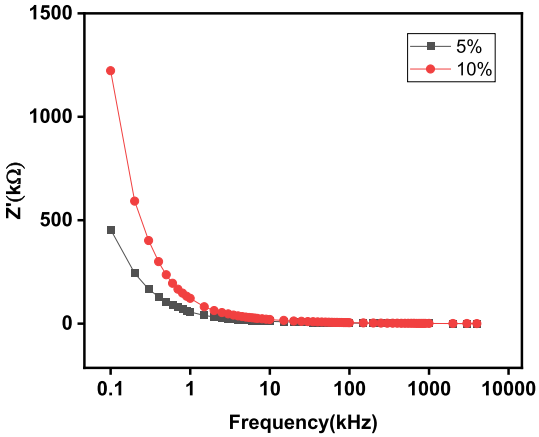

Figure 5. Variation of the real part of impedance as a function of Frequency (kHz) of composite films with 5% and 10% ceramic filler.

Again, the variation of the imaginary part of impedance with frequency is shown in figure 6. Here, the value of Z″ increases rapidly from the negative axis with an increase in frequency and attains a saturation value on further increasing. This may happen due to the presence of some voids. Here no relaxation peak occurs which may be due to the absence of immobile charge carriers.

3.5 *Modulus study*

Figure 7 shows the variation of the real part of modulus (M′) with frequency. For all the samples it shows a very low value (almost zero) at the lower frequency region. It shows a dispersion tending towards M∞ (the asymptotic value of M′ at higher frequencies) and the dispersion shifts towards the higher frequency side as the frequency increases. The asymmetric plot of M′ is because of the stretched exponential character of the relaxation time of the

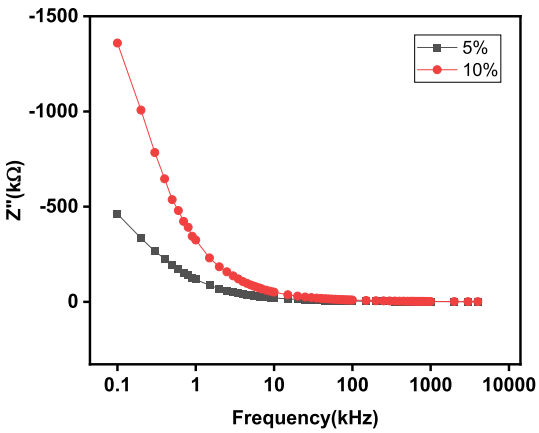

Figure 6. Variation of the imaginary part of impedance as a function of Frequency (kHz) of composite films with 5% and 10% ceramic filler.

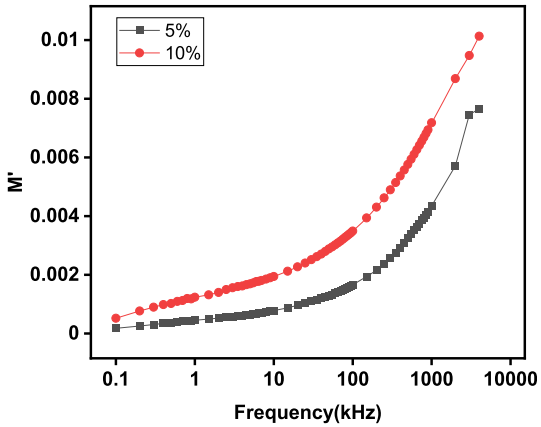

Figure 7. Variation of M′ with the frequency of composite films with 5% and 10% ceramic filler.

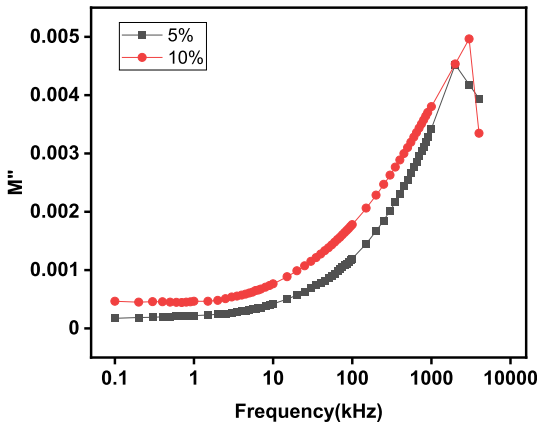

Figure 8. Variation of M″ with the frequency of composite films with 5% and 10% ceramic filler.

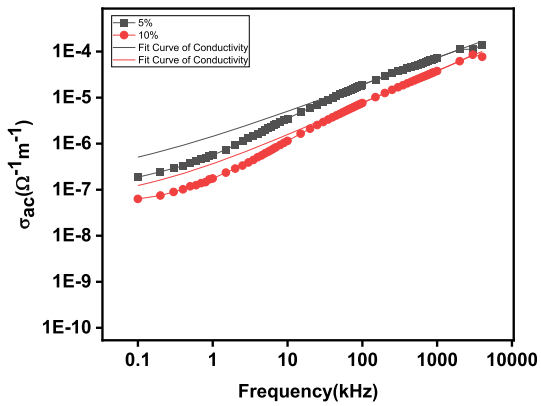

Figure 9. Variation of ac conductivity as a function of the frequency of composite films with 5% and 10% ceramic filler.

material. The monotonous dispersion on increasing frequency may be because of the short-range mobility of charge carriers. This may be due to the lack of restoring

Table 4. Jonscher's power law fitting parameter of ac conductivity versus frequency of composite films at different filler concentrations.

Filler %age	σ_{dc} ($\Omega^{-1}m^{-1}$)	A	n	Goodness of fit (R^2)
5	1.86439E−7	2.14204E−8	0.58945	0.97231
10	6.29986E−8	2.40868E−9	0.69998	0.9712

force governing the mobility of the charge carriers under the action of an induced electric field [33].

On the other hand, the variation of the imaginary part of modulus (M″) can be explained by figure 8. A relaxation mechanism is observed for all the samples of different ceramic filler concentrations. The relaxation peak can be seen in the higher frequency region and it shifts more towards the higher frequency range on an increase in the ceramic concentration. Here the relaxation in all the cases can be considered as a non-Debye type because the asymmetry of peak broadening shows the spread of relaxation times with different time constants [34].

3.6 *Conductivity study*

The conductivity study is done to analyze the conduction mechanism in the composite. The value of ac conductivity can be calculated from the dielectric parameters with the relation [18]

$$\sigma_{ac} = \varepsilon_0 \varepsilon_r \omega \tan\delta \tag{5}$$

where the symbols signify their usual meanings.

Figure 9 explains the variation of ac conductivity with frequency for different concentrations of ceramic in the polymer matrix. Like disordered solids, oxides, and nanocomposites, it shows an increase in conductivity with increasing frequency for all compositions. Figure shows the maximum value at a higher frequency range. This explains the existence of grains with high conductivity and their boundaries exhibiting high resistance [35].

In 2017, Singh [36] showed that doping copper in place of La in perovskite materials increases the electrical conductivity of the sample. In the year 2020, Paramvir Kaur [37] also revealed that the conductivity of the Strontium Titanate increases with Cu doping. In our work, we are also getting a large value of conductivity which indicates that the addition of $PbCuTiO_3$ surely enhanced the electrical conductivity.

The curve can be divided into three parts, i.e. low-frequency region, the plateau region, and the dispersion region. Because of the charge accumulation in the low-frequency region, the conductivity value decreases in this region. The intermediated frequency region is called a plateau region where the dc conductivity leads to the formation of a conducting path in the entire material. The dispersion region is the high-frequency region. In this region, the conductivity is independent of frequency and its value corresponds to that of dc conductivity. This may be because of the random diffusion of the ionic charge carriers. The increase in conductivity is due to the hopping of mobile charge carriers [38]. The frequency dependence of ac conductivity can be explained based on Jonscher's power law [39] stated as

$$\sigma_{ac} = \sigma_{dc} + A\omega^n \tag{6}$$

where A is the temperature pre-exponential factor and n is the dimensionless exponent.

The condition n=0 states that the conductivity is independent of frequency whereas when n<1 the conductivity depends on the frequency [40]. The non-linear fit curve gives the values of σ_{dc}, A, and n which are listed in table 4. The value of n ranges from 0.58 to 0.69 at room temperature which is <1. This indicates the frequency dependence of ac conductivity. Here we can see that the value of conductivity increases on a decrease in ceramic concentration in the polymer matrix as discussed earlier in the impedance study.

4. Conclusion

The ferroelectric ceramic-polymer composites of Cu doped $PbTiO_3$ are successfully prepared by high-temperature solid-state technique and solution casting method. The composites show the tetragonal structure. The dielectric constant was found to be in the range from 12 to 34 for a series of composite films with different ceramic filler percentages with a low loss. Due to the strong doping phase of Cu, it will be a useful material for industrial coating and in solar cell fields. Because of the homogenous distribution of filler in the PMMA polymer matrix, the increasing nature of the dielectric constant can be observed. With increasing frequency, the dielectric constant decrease which explains that all types of polarization exist at low frequency and vanish along with increasing frequency. The value of dielectric constant and electrical ac conductivity increases with a decrease in ceramic concentration. The doping of Cu enhances the conductivity of the composite. The frequency dependence of ac conductivity obeys Jonscher's power law for Cu doped $PbTiO_3$. The modulus study reveals the presence of a hopping mechanism in the composites.

List of symbols

K	Kelvin
k	Kilo (10^3)
ε^*	Complex permitivity
Z^*	Complex impedance
°C	Degree celcius
D	Crystallite size
K	Shape factor (constant) = 0.89
θ	Diffraction angle
λ	Wavelength = 1.5406 Å
$\beta_{1/2}$	Full width of the reflection at half of the maximum intensity
Å	Angstrom
ε	Microstrain
δ	Dislocation density
$\boldsymbol{\varepsilon_r}$	Dielectric constant
tanδ	Dielectric loss
Z'	Real part of the impedance
Z''	Imaginary part of the impedance
M'	Real part of the impedance
M''	Imaginary part of the impedance
σ_{ac}	AC conductivity
ε_0	Absolute permitivity
ε_r	Relative permitivity
ω	Frequency
σ_{dc}	DC conductivity
A	The temperature pre-exponential factor
n	The dimensionless exponent

Declaration

Conflict of interest The authors declare that there is no conflict of interest.

References

[1] Wang J, Pang X, Akinc M and Lin Z 2010 Synthesis and characterization of perovskite $PbTiO_3$ nanoparticles with solution processability. *J. Mater. Chem.* 20: 5945–5949

[2] Zare K, Sadjadi M S, Enhessari M and Khanahmadzadeh S 2009 Synthesis and characterization of $PbTiO_3$ nanopowders by citric acid gel method. *Phys. Theor. Chem.* 6: 9–12

[3] Qiang L, Ma J, Zhang X and Chu J 2008 Preparation and microstructure analysis of Fe-doped $PbTiO_3$ ceramic. *Front. Chem. Eng.* 2: 140–144

[4] Chaudhari V and Bichile G K 2013 Synthesis, structural, and electrical properties of pure $PbTiO_3$ ferroelectric ceramics. *Smart Mater. Struct.* 2013: 9

[5] Han T H, Lee J W, Choi C, Tan S, Lee C and Zhao Y 2019 Perovskite-polymer composite cross-linker approach for highly-stable and efficient perovskite solar cells. *Nat. Commun.* 10: 1–10

[6] Zhang M, Wang M, Yang Z, Li J and Qiu H 2018 Preparation of all-inorganic perovskite quantum dots-polymer composite for white LEDs application. *J. Alloys Compd.* 748: 537–545

[7] Xu Y-F, Yang M-Z, Chen B-X, Wang X-D, Chen H-Y and Kuang D-B 2017 A $CsPbBr_3$ perovskite quantum dot/graphene oxide composite for photocatalytic CO2 reduction. *J. Am. Chem. Soc.* 139: 5660–5663

[8] Yao J, Xiong C, Dong L, Chen C, Lei Y and Chen L 2009 Enhancement of dielectric constant and piezoelectric coefficient of ceramic-polymer composites by interface chelation. *J. Mater. Chem.* 19: 2817–2821

[9] Bai Y, Cheng Z Y, Bharti V, Xu H S and Zhang Q M 2000 High-dielectric-constant ceramic-powder polymer composites. *Appl. Phys. Lett.* 76: 3804–3806

[10] Thomas P, Ravindran R S E and Varma K B R 2012 Dielectric properties of Poly(methyl methacrylate) (PMMA)/$CaCu_3Ti_4O_{12}$ composites. In: *Proc. IEEE Int. Conf. Prop. Appl. Dielectr. Mater.* 1–4

[11] Qin P-L, Lei H-W, Zheng X-L, Liu Q, Tao H and Yang G 2016 Copper-doped chromium oxide hole-transporting layer for perovskite solar cells: Interface engineering and performance improvement. *Adv. Mater. Interfaces.* 3: 1500799

[12] Sahu A K, Satpathy S K and Rout S K 2020 Dielectric and frequency dependent transport properties of gadolinium doped bismuth ferrite. *Trans. Electr. Electron. Mater.* 21: 217–226. https://doi.org/10.1007/s42341-020-00170-7

[13] Satpathy S K, Sen S and Behera B 2017 Dielectric, electrical and magnetic properties of La doped $BiFeO_3$–$PbZrO_3$ composites. *J. Mater. Sci. Mater. Electron.* 28: 9102–9113. https://doi.org/10.1007/s10854-017-6644-9

[14] Sahu A K, Mallick P, Satpathy S K and Behera B 2021 Effect on structural, electrical and temperature sensing behavior of neodymium doped bismuth ferrite. *Adv. Mater. Lett.* 12: 1–7. https://doi.org/10.5185/amlett.2021.071648

[15] Satpathy S K, Mohanty N K and Behera A K 2019 Effect on electrical properties of Gd-doped BiFeO3–PbZrO3. *Iran J. Sci. Technol. Trans. Sci.* 43: 2017–2026. https://doi.org/10.1007/s40995-019-00682-9

[16] Mallick P and Satpathy S K 2021 Synthesis and characterization of Zinc doped Strontium Titanate. *Int. J. Anesth Pain Med.* 7: 37

[17] Mallick P, Sahu A K and Satpathy S K 2022 Investigation on structural, dielectric, thermistor parameters and negative temperature coefficient behaviour of Nd, Gd, and La-doped bismuth ferrite. *Trans. Electr. Electron. Mater.* https://doi.org/10.1007/s42341-021-00379-0

[18] Mohanty D, Satpathy S K, Behera B and Mohapatra R K 2020 Dielectric and frequency dependent transport properties in magnesium doped CuFe2O4 composite. *Mater. Today: Proc.* 33: 5226–5231

[19] Grandgirard J, Poinsot D, Krespi L, Nénon J P and Cortesero A M 2002 Costs of secondary parasitism in the facultative hyperparasitoid Pachycrepoideus dubius: Does host size matter? *Entomol. Exp. Appl.* 103: 239–248

[20] Thutiyaporn Thiwawong KOBT 2013 A humidity sensor based on silver nanoparticles thin film prepared by electrostatic spray deposition process. *Adv. Mater. Sci. Eng.* 2013: 1–7

[21] Fiat Varol S, Babür G, Çankaya G and Kölemen U 2014 Synthesis of sol-gel derived nano-crystalline ZnO thin films as TCO window layer: Effect of sol aging and boron. *RSC Adv.* 4: 56645–56653

[22] Dome K, Podgorbunskikh E, Bychkov A and Lomovsky O 2020 Changes in the crystallinity degree of starch having

different types of crystal structure after mechanical pretreatment. *Polymers* 12: 1–12

[23] Kumari A and Dasgupta Ghosh B 2018 A study of dielectric behavior of manganese doped barium titanate–polyimide composites. *Adv. Polym. Technol.* 37: 2270–2280

[24] Arya A and Sharma A L 2018 Effect of salt concentration on dielectric properties of Li-ion conducting blend polymer electrolytes. *J. Mater. Sci. Mater. Electron.* 29: 17903–17920

[25] Rayssi C, El Kossi S, Dhahri J and Khirouni K 2018 Frequency and temperature-dependence of dielectric permittivity and electric modulus studies of the solid solution Ca0.85Er0.1Ti1-: XCo4 x /3O3 ($0 \leq x \leq 0.1$). *RSC Adv.* 8: 17139–17150

[26] Paquin F, Rivnay J, Salleo A, Stingelin N and Silva C 2015 Multi-phase semicrystalline microstructures drive exciton dissociation in neat plastic semiconductors. *J. Mater. Chem. C* 3: 10715–10722

[27] Pascariu V, Avadanei O, Gasner P, Stoica I, Reverberi A P and Mitoseriu L 2013 Preparation and characterization of PbTiO3–epoxy resin compositionally graded thick films. *Phase Transit.* 86: 715–725

[28] Tamboli M S, Palei P K, Patil S S, Kulkarni M V, Maldar N N and Kale B B 2014 Polymethyl methacrylate (PMMA)–bismuth ferrite (BFO) nanocomposite: low loss and high dielectric constant materials with perceptible magnetic properties. *Dalton Trans.* 43: 13232–13241

[29] Singh P 2014 Ferroelectric polymer-ceramic composite thick films for energy storage applications. *AIP Adv.* 4: 87117

[30] Beena P and Jayanna H S 2019 Dielectric studies and AC conductivity of piezoelectric barium titanate ceramic polymer composites. *Polym. Polym. Compos.* 27: 619–625

[31] Kobayashi Y, Tanase T, Tabata T, Miwa T and Konno M 2008 Fabrication and dielectric properties of the BaTiO3-polymer nano-composite thin films. *J. Eur. Ceram. Soc.* 28: 117–122

[32] Habib A, Stelzer N and Haubner R 2014 Fabrication of BaTiO3-PMMA polymer nanocomposite thin/thick films and their dielectric properties. *Solid State Phenom.* 151: 108–112

[33] Thakur S, Rai R, Bdikin I and Valente M A 2016 Impedance and modulus spectroscopy characterization of Tb modified Bi0.8A0.1Pb0.1Fe0.9Ti0.1O3 ceramics. *Mater. Res.* 19: 1–8

[34] Bag S, Das P and Behera B 2017 AC impedance spectroscopy and conductivity studies of Dy doped Bi4V2O11 ceramics. *J. Theor. Appl. Phys.* 11: 13–25

[35] Radoń A, Łukowiec D, Kremzer M, Mikuła J and Włodarczyk P 2018 Electrical conduction mechanism and dielectric properties of spherical shaped Fe_3O_4 nanoparticles synthesized by co-precipitation method. *Materials (Basel, Switzerland).* 11: 735

[36] Singh N K, Yadav M K and Fernandez C 2017 Electro catalytic properties of La1-xCuxCoO3 ($0 \leq x \leq 0.8$) film electrodes prepared by Malic Acid sol-gel method at pH = 3.75. *Int. J. Electrochem. Sci.* 12: 7128–7141

[37] Kaur P and Singh K 2020 Structural, thermal and electrical study of copper doped strontium zirconate. *Ionics* 26: 6233–6244

[38] Kumar S, Pal J, Kaur S, Malhi P S, Singh M and Babu P D 2019 The structural and magnetic properties, non- Debye relaxation and hopping mechanism in solutions. *J. Asian Ceram. Soc.* 7: 133–140

[39] Satpathy S K, Mohanty N K, Behera A K and Behera B 2014 Dielectric and electrical properties of 0.5(BiGd0.05Fe 0.95O3)-0.5(PbZrO3) composite. *Mater. Sci.-Pol.* 32: 59–65

[40] Singh S, Katyal S and Goswami N 2019 Dielectric and electrical study of zinc copper ferrite nanoparticles prepared by exploding wire technique. *Appl. Phys. A.* 125: 1–14